1971

Surface plasmon-longitudinal optical phonon contribution to the reflectivity of n-type InSb

William Eugene Anderson

Department: Physics

165

SURFACE PLASMON-LONGITUDINAL OPTICAL PHONON

CONTRIBUTION TO THE REFLECTIVITY OF N-TYPE InSb

by

WILLIAM EUGENE ANDERSON, 1946-

A DISSERTATION

Presented to the Faculty of the Graduate School of the

UNIVERSITY OF MISSOURI - ROLLA

In Partial Fulfillment of the Requirements for the Degree

DOCTOR OF PHILOSOPHY

in

PHYSICS

1971

Ralph W. Alexander Jr.
ADVISOR

David L. Sch...

W. F. Parks

Wayne E. Tefft

W. J. James

Don M. Sparlin

ABSTRACT

The reflectivity of n-type InSb has been measured in the far infrared. The doping of the samples was such that the free-carrier plasma frequency was near the longitudinal optical phonon frequency. The results suggest that samples with a sufficiently thick damage layer show effects due to surface plasmons. The results also indicate that the surface plasma excitations are coupled to the phonons.

A simple model of this coupling is presented which agrees qualitatively with the observed reflectivity. A somewhat more rigorous theory of the coupling is also presented.

ACKNOWLEDGEMENT

The author wishes to acknowledge the help of Dr. Ralph W. Alexander, Jr. in this study. His experience, knowledge, and advice were invaluable in all phases of this work.

The original idea to study this phenomenon belongs to Dr. Robert J. Bell. Dr. William F. Parks' contributions to the theoretical aspects of the problem are greatly appreciated.

The author also wishes to thank Joe M. Blea for his help with the Michelson interferometer. This work was supported by the Air Force Office of Scientific Research under Contract No. AFOSR-F-44620-69-C-D122.

TABLE OF CONTENTS

LIST OF ILLUSTRATIONS

LIST OF ILLUSTRATIONS (CONTINUED)

LIST OF TABLES

I. INTRODUCTION

The coupling of surface plasmons to optical phonons is the subject of this thesis. Far infrared reflectivity measurements were made on n-type InSb crystals with concentrations of 1.43, 2.60, and 3.96 x 10^{17} tellurium impurities per cm^3. Since both bulk and surface plasmons can couple with optical phonons, the surface plasmon frequency should be significantly different from the bulk plasmon frequency to facilitate differentiating surface and bulk effects. The relationship between the bulk and surface plasmon frequencies (ω_P and ω_{SP}, respectively) is given by:

$$\omega_{SP} = \omega_P/(1 + \varepsilon/\varepsilon_\infty)^{1/2} \qquad (1)$$

where ε_∞, the high frequency dielectric constant, is equal to 15.68 for InSb and ε is the dielectric constant of the material bounding the InSb. If the bounding medium is a thick layer of intrinsic (or depleted) InSb, then ω_{SP} would equal $\omega_P/\sqrt{2}$. Therefore, a spark cutter was used to create a damage layer in which the electron mobility was significantly reduced because of the additional trap sites. The observed reflectivity of this n-type InSb-damaged InSb interface is compared with a simple, coupled surface plasmon-optical phonon model.

The existence of surface plasmons was first suggested by Ritchie[1] and subsequently verified in metals by others.[2-7] Reflectivity measurements on smooth metal surfaces will not show surface-plasmon effects because the incident photon has less momentum than the corresponding surface plasmon of the same energy. However, anomalies, first observed by Wood[8] in the intensity of p-polarized light from metal diffraction gratings, were explained by Ritchie *et al*.[9] in terms of second and possibly higher order surface plasmon-grating interactions. The periodic density variation in the region of the surface allows the grating to absorb momentum perpendicular to the grating lines in multiples of h/d where d is the spacing of the grating lines.

Tsui[10] first detected surface plasmons in degenerate semiconductors. He observed structure in d^2I/dV^2 as a function of voltage for a semiconductor-metal-tunnel junction which corresponded to an increase in conductance at bias voltages near the surface plasmon energy, 69 mev or 550 cm^{-1} (for n-type GaAs with 6.5 x 10^{18} free carriers per cm^3). Tsui's results were explained by Ngai, Economou and Cohen[11] and Ngai and Economou.[12] Marschall, Fischer, and Queisser[13] were the first to observe surface plasmons in reflectance studies on semiconductors. Following the grating idea of Ritchie,[9] they observed the surface plasmon contribution to the reflectivity of an n-type InSb grating with a surface plasmon frequency of 700 cm^{-1}.

Bulk plasmon-phonon coupling has been observed in semiconductors by several workers.[14-17] The results of these experiments are in excellent agreement with a theory developed by Varga[18] and Singwi and Tosi.[19] This coupling of the bulk plasmon to the longitudinal optical phonon suggests that a similar coupling between surface plasmons and phonons might be possible if the surface plasmon frequency is near the phonon frequencies ($\simeq$190 cm^{-1} for InSb). The first report of surface plasmon-phonon coupling was made by Anderson, Alexander, and Bell.[20] A theoretical discussion of this coupling was presented by Parks,[21] Chiu and Quinn,[22] and Wallis and Brion.[23]

II. EXPERIMENTAL PROCEDURE

Far-infrared reflectivity measurements were obtained using a Twyman-Green interferometer, the FS-720 made by RIIC and supplied by Beckman-Instruments, Inc. The source was a medium-pressure, mercury-arc lamp, the Philips HPK-125W. Reflectivity measurements were made in the 10 to 400 cm^{-1} range using a mylar beamsplitter of thickness 6μm. Resolution of approximately 2 wave numbers with apodization was achieved. The detectors used were a Golay cell manufactured by Unicam Ltd. in Great Britain and a gallium-doped germanium bolometer made by Texas Instruments. A polished aluminum mirror was used as a background for the reflectivity of the smooth samples. The TR-5 A.T.R. (attenuated total reflection) unit, shown in Fig. 1 and made by RIIC, was used strictly as a sample holder for the reflectivity measurements. The light reaching the sample was uncollimated. The angle of incidence could be varied from 25° to 68°.

A spark cutter was used for cutting the samples to fit the sample holder (∿1 cm x 1 cm) and for cutting gratings on the surface (for reasons discussed in Chapter IV). The spark cutting operation involved a 2 mil stainless steel wire mounted parallel to the sample surface. The wire at approximately 120 volts potential (with respect to the sample) was slowly lowered to the sample surface. The electrons bombarding the crystal surface locally heat and vaporize the crystal material. A micrometer drive was used to adjust the spacing between cuts. Reflectivity backgrounds for the grating-cut samples were obtained by evaporating a thin layer of gold on the grating

FIGURE 1

OPTICAL DIAGRAM OF TR-5 A.T.R. UNIT. The unit was used as a sample holder for reflectivity measurements.

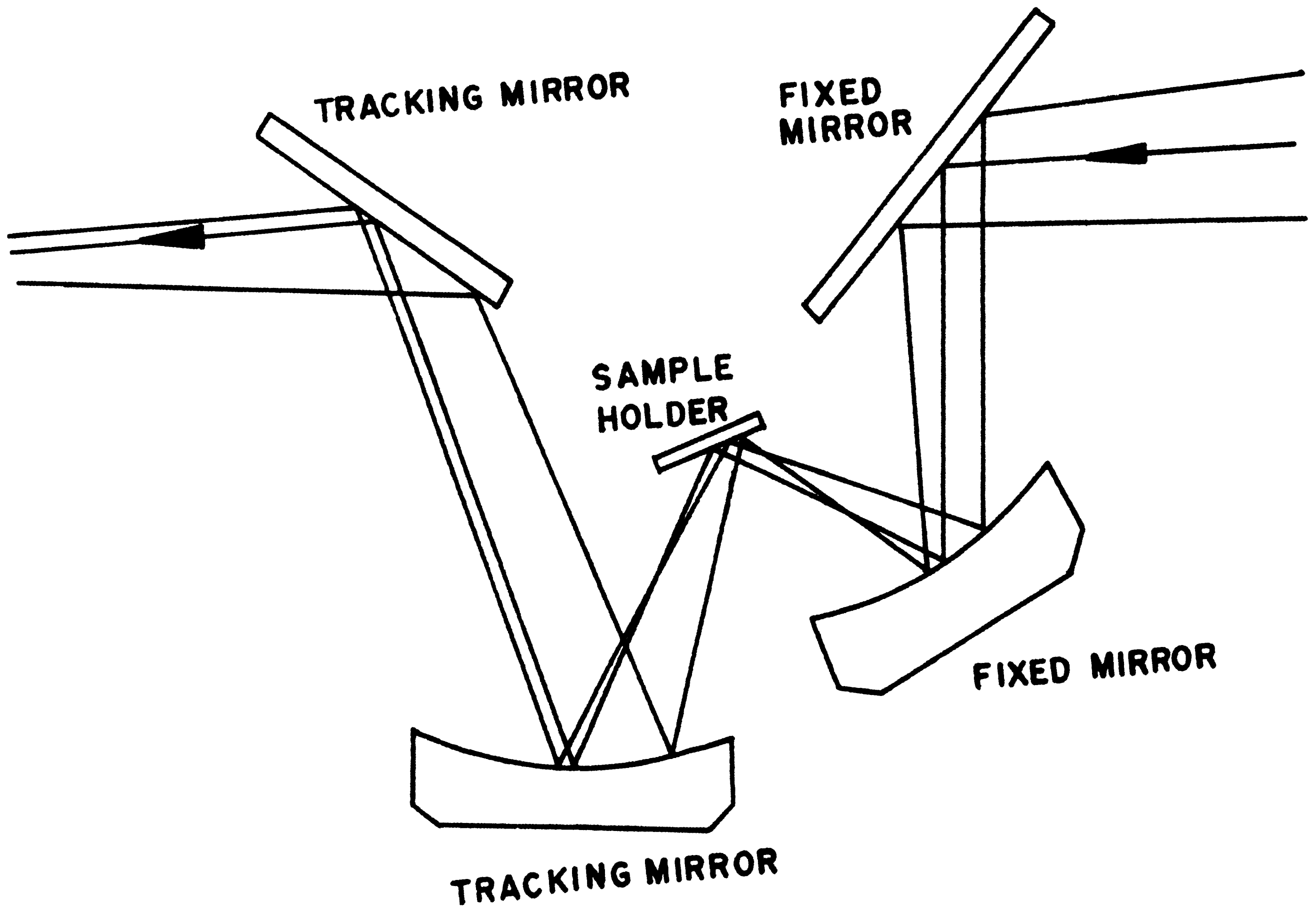
TRACKING MIRROR
FIXED
MIRROR
SAMPLE
HOLDER
FIXED MIRROR
TRACKING MIRROR

Figure 1

surface. A wire grid polarizer with a polyethylene substrate purchased from the Perkin Elmer Corporation was used for polarization studies.

The Te-doped InSb samples were supplied by the Monsanto Company. The free electron concentrations were 1.43, 2.60, and 3.96 x 10^{17} per cm^3. Their mobilities were about 7.3 x 10^4 cm^2/volt-sec. The polished faces of the slices were parallel to the (111) planes of the crystal. All measurements were made at room temperature.

III. BULK PLASMON-PHONON COUPLING

A plasma oscillation is a collective longitudinal excitation of the free electrons in a material. A quantized plasma oscillation is called a plasmon. The plasma frequency, ω_p, is given by:

$$\omega_p^{\,2} = 4\pi N e^2 / m^* \varepsilon_\infty , \qquad (2)$$

where N is the free carrier concentration, e the charge on the electron, and the effective mass is denoted by m*. The plasma frequency is to first order independent of the wave vector.[24]

The problem of bulk plasmon-longitudinal optical phonon coupling was first treated by Varga[18] and Singwi and Tosi[19] and subsequently verified experimentally by several workers.[14-17] The main point of Varga's approach is that the polarizability of the electrons and ions are additive in the self-consistent-field theory. As a consequence of this, the total dielectric function of a degenerate semiconductor in the long wavelength (or local) approximation is:

$$\varepsilon(0,\omega) = \varepsilon_\infty + \frac{\varepsilon_o - \varepsilon_\infty}{1 - (\omega/\omega_o)^2} - \frac{\varepsilon_\infty \omega_p^{\,2}}{\omega^2} \qquad (3)$$

where ε_∞ and ε_o are the high frequency and damped dielectric constants respectively and ω_o is the transverse optical (TO) mode frequency. Bell and McMahon[17] used this dielectric to explain the reflectivity of

InSb and CdS in the far infrared. Fig. 2 (from McMahon[25]) shows the excellent agreement between theory and experiment where Eqn. 3 has been modified to include damping as follows:

$$\varepsilon(0,\omega) = \varepsilon_\infty + \frac{\varepsilon_o - \varepsilon_\infty}{1 - (\omega/\omega_o)^2 - i\omega\Gamma/\omega_o^2} - \frac{\varepsilon_\infty \omega_p^2}{\omega^2 + i\omega/\tau}, \tag{4}$$

τ and Γ represent the electron and phonon damping respectively. The effect of the presence of the plasma on the reflectivity is shown in Fig. 2. The minimum in the reflectivity for the undoped sample, shown in Fig. 3, is near 190 cm^{-1}, the longitudinal optical (LO) phonon frequency. The addition of the plasmons, which are longitudinal excitations that can couple to the LO phonons, results in the forming of two normal modes, ω_- and ω_+. The TO phonons remain unchanged since, as Ferrel[26] has pointed out, the plasmons cannot couple to transverse electromagnetic fields. An expression for the values of ω_- and ω_+ can be derived directly from Eqn. 4 by noting that the longitudinal solutions are those for which $Re(\varepsilon(0,\omega))$ vanish. Letting $Re(\varepsilon(0,\omega))$ equal zero (and neglecting damping), it follows that:

$$(\omega_\pm)^2 = 1/2\ (\omega_{LO}^2 + \omega_p^2) \pm 1/2\ [(\omega_{LO}^2 - \omega_p^2)^2 + 4\omega_L^2\omega_p^2(1 - \varepsilon_\infty/\varepsilon_o)]^{1/2} \tag{5}$$

where ω_{LO} is the LO phonon frequency ($\omega_{LO} = \omega_{TO}(\varepsilon_o/\varepsilon_\infty)^{1/2}$). The minima in the reflectivity (see Fig. 2) for InSb with 3.96 x 10^{17} free

FIGURE 2

REFLECTANCE VERSUS WAVE NUMBER OF A POLISHED CRYSTAL OF N-TYPE InSb ($N=3.96\times10^{17}$). The x's are the data points of McMahon.[25] The solid curve is the calculated reflectivity from Eqn.4. The angle of incidence is 30°.

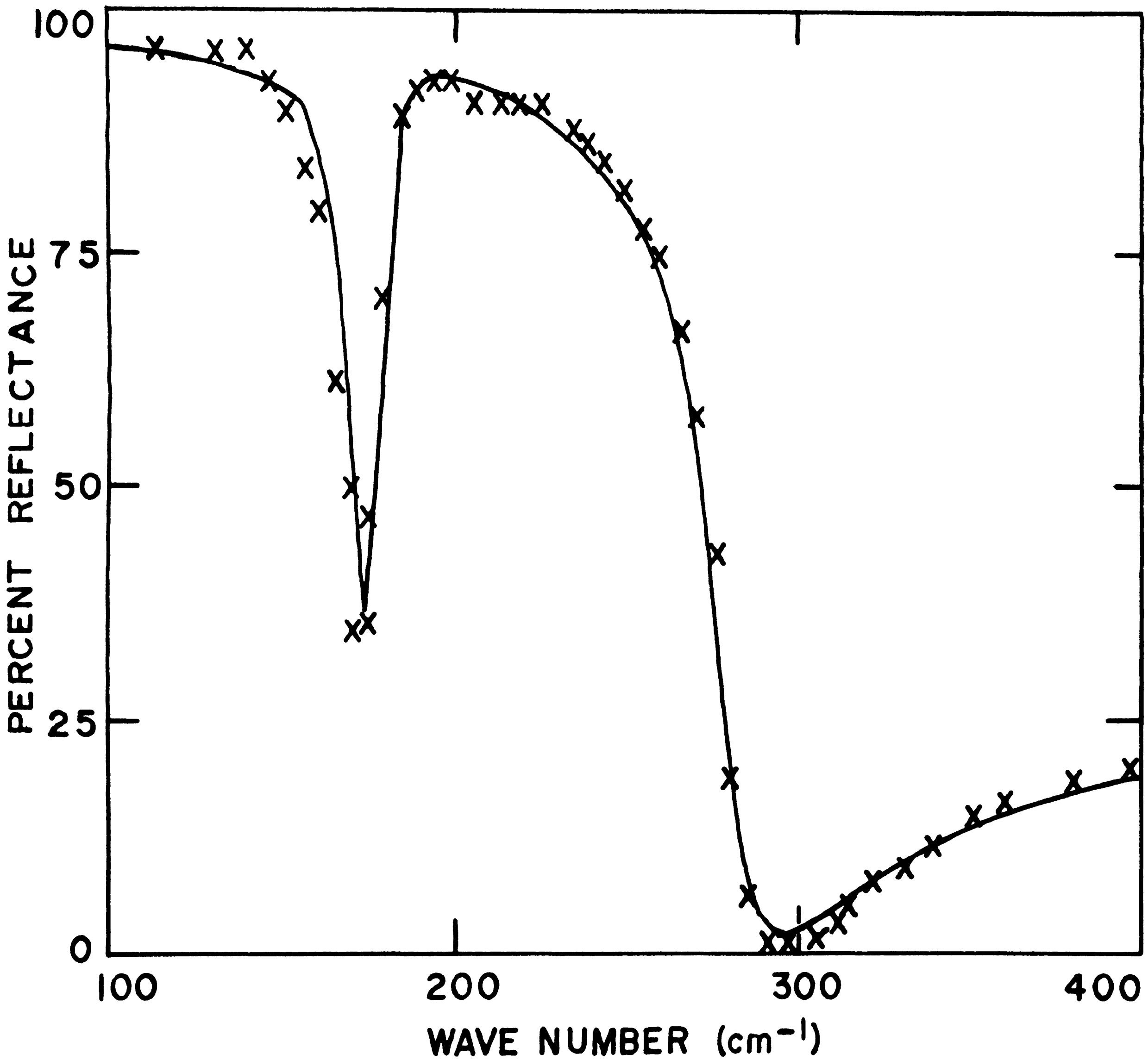
100
75
50
25
0
PERCENT REFLECTANCE
100
200
300
400
WAVE NUMBER (cm⁻¹)

Figure 2

FIGURE 3

REFLECTANCE VERSUS WAVE NUMBER OF AN UNDOPED CRYSTAL OF InSb. The curve is calculated from Eqn.4 with $N=0$. The angle of incidence is 30°.

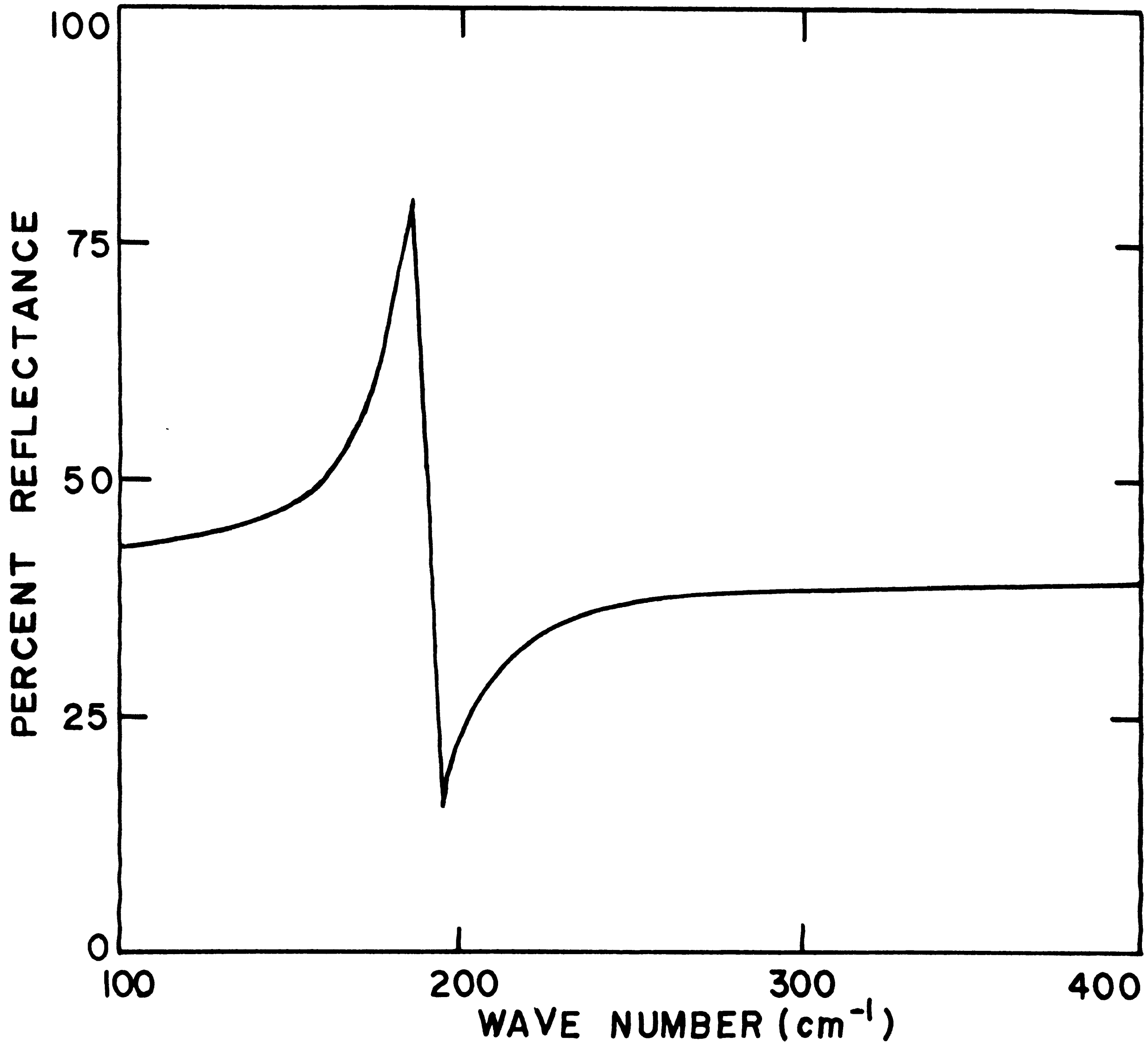
PERCENT REFLECTANCE
0
25
50
75
100
100
200
300
400
WAVE NUMBER (cm⁻¹)

Figure 3

carriers per cm^3 are at 170 and 290 cm^{-1}. The two normal longitudinal modes from Eqn. 5 are at 173 and 295 cm^{-1}. Therefore, the minima in the reflectivity lie very close to ω_- and ω_+ (Eqn. 5 gives the zero's of $\varepsilon(0,\omega)$ whereas the reflectivity minima occur where $\varepsilon(0,\omega)=1$).

An alternative method of deriving Eqn. 5 is to consider the problem of two harmonic oscillators of masses M_1, M_2 and spring constants K_1 and K_2 connected to each other by a spring of constant K_3. The two normal modes for this system are known to be[27]

$$(\omega_\pm)^2 = (\omega_1^2 + \omega_2^2)/2 \pm \{(\omega_1^2 - \omega_2^2)^2 + 4K_3^2/M_1M_2\}^{1/2}/2. \tag{6}$$

The resonant frequency of oscillation of $M_1(M_2)$ if $M_2(M_1)$ is held fixed is $\omega_1(\omega_2)$ where:

$$\omega_1^2 = (K_1 + K_3)/M_1 \tag{7}$$

and

$$\omega_2^2 = (K_2 + K_3)/M_2. \tag{8}$$

If the following identifications are made:

$$\omega_1 = \omega_{LO} , \tag{9}$$

$$\omega_2 = \omega_p \ , \tag{10}$$

and

$$K_3^{\ 2} = K_1 K_2 \ (1 - \varepsilon_\infty/\varepsilon_o) \ , \tag{11}$$

then Eqn. 6 becomes identical to Eqn. 5. The strength of the coupling between the bulk plasmons and LO phonons is given by Eqn. 11. If the ions do not contribute to the dielectric response ($\varepsilon_o = \varepsilon_\infty$), then the effective spring constant coupling the modes is zero. This model of the coupling between phonons and bulk plasmons will be useful in discussing the surface plasmon-phonon coupling.

IV. SURFACE PLASMON-PHONON COUPLING

A. Surface Plasmons

Surface plasmons are collective oscillations of the electron charge density confined to the interface between a free carrier plasma and a dielectric medium. The fields associated with this surface charge density oscillation decay exponentially on both sides of the interface.

The relationship between the surface plasmon frequency and the plasmon frequency for a semiconductor can be found by generalizing a treatment by Stern and Ferrell.[28] The semiconductor is approximated by a semi-infinite, ideally nonabsorptive, dielectric medium. It is assumed that the electron gas can be described by the ideal plasma dielectric function:

$$\varepsilon_p(\omega) = \varepsilon_\infty(1 - \omega_p^{\,2}/\omega^2) \tag{12}$$

where ε_∞ is the high frequency dielectric constant of the semiconductor. If no external charges are present, the normal component of the electric displacement vector should be continuous in passing across the interface from the electron gas into the dielectric medium. Therefore,

$$\varepsilon_p(\omega) = -\,\varepsilon\ , \tag{13}$$

where ε is the dielectric constant of the bounding medium.

Substituting Eqn. 12 into Eqn. 13 and solving for the resonant frequency of the surface waves, ω_{sp}, results in

$$\omega_{sp} = \omega_p/(1 + \varepsilon/\varepsilon_\infty)^{1/2}. \tag{14}$$

For an InSb-vacuum interface, the surface plasmon frequency would be approximately the same as the plasmon frequency because ε_∞ equals 15.68 for InSb. However, if the bounding medium is a thick layer of germanium (with ε = 16) or depleted (or intrinsic) InSb, then ω_{sp} is approximately equal to $\omega_p/\sqrt{2}$.

A surface plasmon cannot be excited directly by a photon because a photon has less momentum than the surface plasmon of the same energy as shown in Fig. 4, a dispersion plot for surface plasmons from Fuchs and Kliewer[29] (assuming a free-electron gas in the local approximation). Ritchie[9] has shown that a grating ruled on the surface of the crystal can supply momentum in multiples of h/d where d is the grating spacing. This additional momentum can aid a second order, photon-surface plasmon-grating interaction for light polarized perpendicular to the grating lines. For light polarized parallel to the grating lines, no interaction is possible. Since any static variation in the electron density in the vicinity of the surface can supply momentum, surface plasmons can be observed in reflectivity measurements of rough surfaces. In semiconductors there also exists the possibility that the surface plasmons can interact with the optical phonons similar to the

FIGURE 4

SURFACE PLASMON FREQUENCY VERSUS WAVE VECTOR FOR A FREE ELECTRON GAS IN THE LOCAL APPROXIMATION. The calculated dispersion curve is from Fuchs and Kliewer.[29] The frequency scale is labeled in units of ω_{SP} and the wave vector scale is labeled in units of ω_{SP}/c.

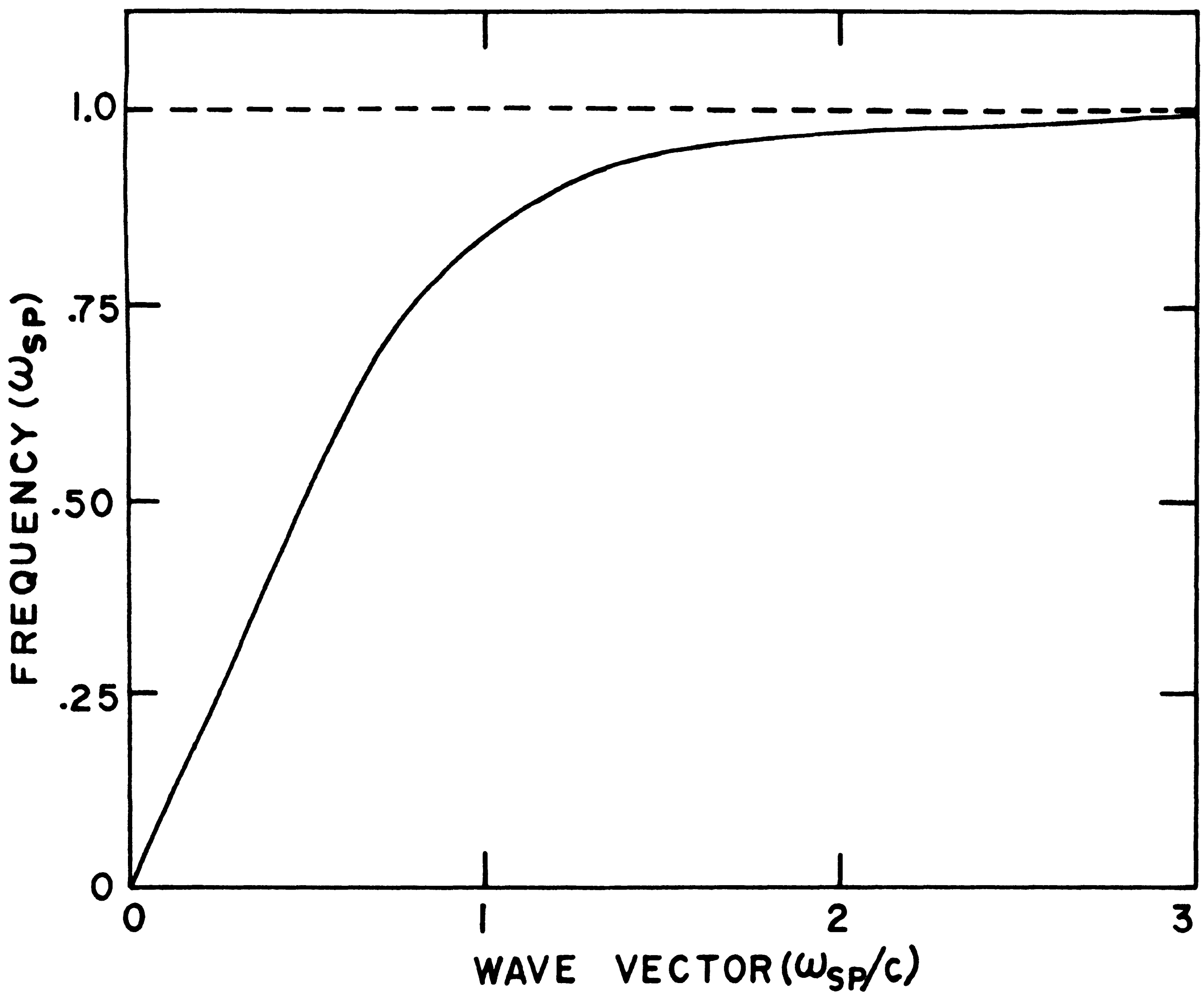

Figure 4

bulk plasmom-phonon coupling

B. Surface Plasmon-Phonon Coupling.

A dispersion relationship for surface waves on a semiconductor-dielectric interface (including lattice contributions) can be derived from Maxwell's equations. This derivation follows that of Parks.[21] The interface is at $z = 0$ with the semiconductor occupying the $z>0$ semi-infinite space.

Maxwell's equations are (with μ, the magnetic permeability, equal to one);

$$\nabla \times \vec{E} = -\frac{1}{c}\frac{\partial \vec{B}}{\partial t}, \tag{15}$$

$$\nabla \times \vec{B} = \frac{4\pi \vec{J}}{c} + \frac{1}{c}\frac{\partial \vec{D}}{\partial t}, \tag{16}$$

$$\nabla . \vec{B} = 0 \tag{17}$$

and

$$\nabla . \vec{D} = 4\pi\delta\rho, \tag{18}$$

where $\delta\rho$ is the deviation of the electron charge density from the equilibrium, free electron charge density. Since $\vec{J} = \sigma(\omega)\vec{E}$,

$$\nabla . \vec{J} = \sigma(\omega)\nabla . \vec{E}. \tag{19}$$

From the continuity relationship for charge and current it follows that:

$$\nabla.\vec{J} + \frac{\partial\delta\rho}{\partial t} = 0. \tag{20}$$

Substituting Eqn. 19 into Eqn. 20, one obtains:

$$\sigma(\omega)\nabla.\vec{E} = \frac{\partial\delta\rho}{\partial t} . \tag{21}$$

Assuming that $\vec{D}$, $\vec{E}$, $\vec{J}$ and $\delta\rho$ vary with time as $e^{-i\omega t}$, then

$$\nabla.\vec{E} = \frac{i\omega\delta\rho}{\sigma(\omega)} \tag{22}$$

or since $\nabla.\vec{D} = 4\pi\delta\rho$, then

$$\nabla.\vec{D} = -\frac{4\pi i\sigma(\omega)}{\omega}\nabla.\vec{E}. \tag{23}$$

Since $\vec{D} = \varepsilon_c(\omega)\vec{E}$ (where $\varepsilon_c(\omega)$ is the dielectric constant of the undoped InSb), from Eqn. 23 it follows that:

$$\nabla.[\varepsilon_c(\omega) + \frac{4\pi i\sigma(\omega)}{\omega}]\vec{E} = 0. \tag{24}$$

Therefore,

$$\nabla . \vec{D}_M = 0 , \tag{25}$$

where $\vec{D}_M$ (the total electric displacement of the semiconductor including the polarization of the free electrons) is given by the relation:

$$\vec{D}_M = (\varepsilon_c(\omega) + 4\pi i \sigma(\omega)/\omega)\vec{E} . \tag{26}$$

From Eqn. 25 and Eqn. 26 it is apparent that either

$$\varepsilon_c(\omega) + 4\pi i \sigma(\omega)/\omega = 0 \tag{27}$$

or

$$\nabla . \vec{E} = 0 . \tag{28}$$

Assuming the latter and requiring E to vary exponentially as $e^{-\alpha z}$ for z>0 one obtains:

$$i(K_x E_x + K_y E_y) - \alpha E_z = 0 . \tag{29}$$

From Eqn. 15 and Eqn. 16, one finds that:

$$-i\frac{c}{\omega}\nabla \times \nabla \times \vec{E} = 4\pi\vec{J}/c - i\omega\varepsilon_c(\omega)\vec{E}/c . \tag{30}$$

Since $\nabla.\vec{E} = 0$,

$$\nabla^2\vec{E} + (\omega^2\varepsilon_c(\omega) + 4\pi i\sigma(\omega)\omega)\vec{E}/c^2 = 0 \tag{31}$$

or

$$-K_x^2 - K_y^2 + \alpha^2 + \omega^2(\varepsilon_c(\omega) + 4\pi i\sigma(\omega)/\omega)/c^2 = 0. \tag{32}$$

This is equivalent to

$$-K_x^2 - K_y^2 + \alpha^2 + \omega^2\varepsilon_M(\omega)/c^2 = 0 \tag{33}$$

where $\varepsilon_M(\omega)$ is the total dielectric constant of the semiconductor.

A similar argument for the dielectric layer (with dielectric constant equal to $\varepsilon(\omega)$) results in the following relations:

$$iK_x'E_x' + iK_y'E_y' + \alpha'E_z' = 0 \tag{34}$$

and

$$-K_x'^2 - K_y'^2 + \alpha'^2 + \varepsilon(\omega)\omega^2/c^2 = 0, \tag{35}$$

where the primes denote quantities for z<0.

Since (from Eqn. 25) the normal component of $\vec{D}_M$ is continuous at z = 0,

$$\varepsilon(\omega)E_z'(0) = \varepsilon_M(\omega)E_z(0) \tag{36}$$

and

$$K_x = K_x'. \tag{37}$$

where the coordinate system is orientated in such a way that E_y is set equal to zero. The tangential components of $\vec{E}$ are also continuous at the interface:

$$E_x'(0) = E_x(0) \tag{38}$$

and

$$E_y'(0) = E_y(0) = 0. \tag{39}$$

Eqn. 34 now becomes

$$i\, K_x E_x(0) + \frac{\varepsilon_M(\omega)\alpha'}{\varepsilon(\omega)} E_z(0) = 0. \tag{40}$$

Comparing Eqn. 40 with Eqn. 29, it is evident that:

$$\alpha = -\alpha' \varepsilon_M(\omega)/\varepsilon(\omega). \tag{41}$$

Eqn. 35 becomes

$$-K_x^2 + \alpha^2 (\varepsilon(\omega))^2/(\varepsilon_M(\omega))^2 + \varepsilon(\omega)\omega^2/c^2 = 0. \tag{42}$$

Combining Eqn. 33 and Eqn. 35, a little algebra results in the dispersion relations for the surface modes:

$$c^2 K_x^2 = \omega^2 \varepsilon(\omega)\varepsilon_M(\omega)/(\varepsilon(\omega) + \varepsilon_M(\omega)) \tag{43}$$

and

$$c^2\alpha^2 = -\omega^2 (\varepsilon_M(\omega))^2/(\varepsilon(\omega) + \varepsilon_M(\omega)). \tag{44}$$

For nonradiative modes, both K_x and α must be real (this is equivalent to an oscillating wave confined to the interface and decaying exponentially away from the interface). If K_x is real but α is imaginary, the mode is radiative since the fields vary sinusoidally away from the surface.

Scattering from a rough surface will allow the excitation of large K modes. The frequency of these large wave vector modes can be found from Eqn. 43 by noting that $\varepsilon(\omega) + \varepsilon_M(\omega)$ must approach zero.

For the case of a semiconductor bounded by a thick damaged (or intrinsic) layer of the same material, $\varepsilon(\omega)$ and $\varepsilon_M(\omega)$ are given by:

$$\varepsilon(\omega) = \varepsilon_\infty + \frac{\varepsilon_o - \varepsilon_\infty}{1 - (\omega/\omega_o)^2 - i\omega\Gamma/\omega_o^2} \tag{45}$$

and

$$\varepsilon_M(\omega) = \varepsilon_\infty + \frac{\varepsilon_o - \varepsilon_\infty}{1 - (\omega/\omega_o)^2 - i\omega\Gamma/\omega_o^2} - \frac{\varepsilon_\infty \omega_p^2}{\omega^2 + i\omega/\tau} . \tag{46}$$

Setting $\varepsilon(\omega) + \varepsilon_M(\omega)$ equal to zero, the frequencies for the large wave vector modes (ω_-, ω_+) are:

$$\omega_\pm^2 = (\omega_{LO}^2 + \omega_p^2/2)/2 \pm [(\omega_{LO}^2 - \omega_p^2/2)^2 + 2\omega_{LO}^2\omega_p^2(1-\varepsilon_\infty/\varepsilon_o)]^{1/2}/2. \tag{47}$$

or

$$\omega_\pm^2 = \frac{\omega_{LO}^2 + \frac{\omega_p^2}{2}}{2} \pm \left\{\left(\omega_{LO}^2 + \frac{\omega_p^2}{2}\right)^2 - 2\omega_{LO}^2\,\omega_p^2\frac{\varepsilon_\infty}{\varepsilon_o}\right\}^{1/2}/2$$

This is identical to Eqn. 5 (the equation for the normal modes of the coupled bulk plasmon-longitudinal optical phonon system) with ω_p in that case replaced by $\omega_p/\sqrt{2}$. In Chapter II a coupled spring model was introduced to explain the coupling of bulk plasmons to longitudinal optical phonons. If in Eqn. 10 ω_2 is set equal to $\omega_p/\sqrt{2}$ (the surface plasmon frequency) instead of ω_p, the normal modes of the coupled spring model will agree with Eqn. 47. Chiu and Quinn[22] and Wallis and Brion[23] derived an equation for the normal modes identical to Eqn. 47 if ω_{SO} is substituted for ω_{LO} where ω_{SO} is the surface optical phonon frequency. There is some question about whether phonons confined to a damaged layer-semiconductor interface can properly be called surface phonons.

Fig. 5 is a dispersion plot (using Eqn. 43) for n-type InSb with a free-carrier concentration of 3.96×10^{17}. The modes are labelled nonradiative (radiative) if α (from Eqn. 44) is real (imaginary). Radiative modes correspond to a transmission or reflection of incident energy whereas nonradiative modes correspond to an absorption of energy to excite a surface wave. The radiation from this excited surface wave might be detected at a different angle than the specularly reflected light. There should be a reflectivity minimum for each nonradiative mode (assuming momentum is conserved between the incident photon and the excited surface wave). If the surface is rough, the minima should correspond to ω_- and ω_+ (Eqn. 47), the frequencies of the large wave vector nonradiative modes (see Fig. 5). The extremely narrow nonradiative mode that lies between ω_- and ω_+ in Fig. 5 corresponds to ω_o, the transverse optical phonon frequency at which both $\varepsilon(\omega)$ and $\varepsilon_M(\omega)$ approach infinity. The sharp minimum in the reflectivity corresponding to this mode may be difficult to resolve, and in fact was not observed in this study.

FIGURE 5

SURFACE MODE FREQUENCY VERSUS WAVE VECTOR FOR A DAMAGED InSb-N-TYPE InSb INTERFACE WITH 3.96×10^{17} FREE CARRIERS PER CM^3. The calculated curve is from Eqn.43. The solid lines represent nonradiative modes while the dashed lines are the radiative modes. The frequency scale is in units of ω_p and the wave vector scale is in units of ω_p/c.

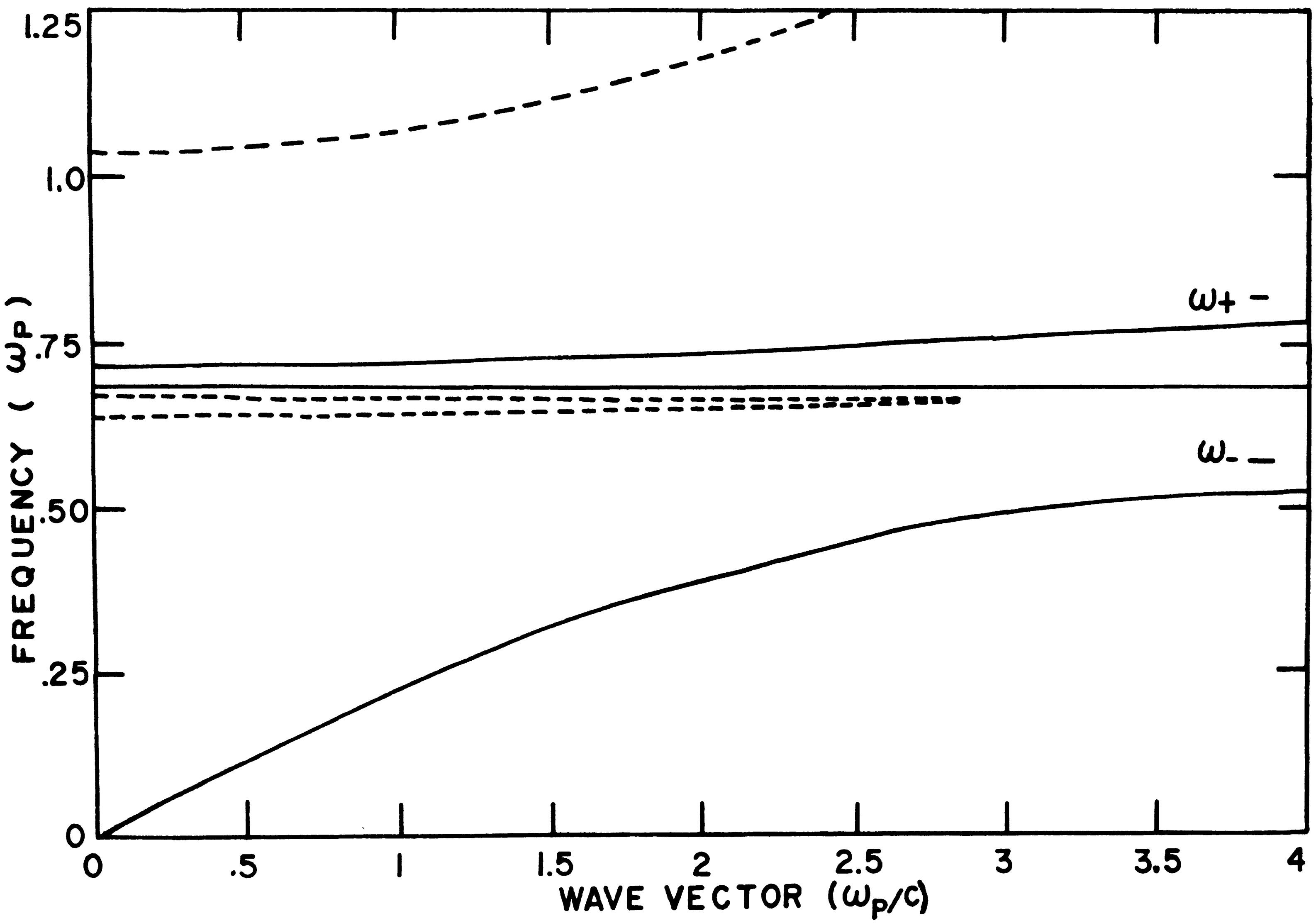

1.25
1.0
.75
.50
.25
0
FREQUENCY (ω_p)
ω_+
ω_-
0
.5
1
1.5
2
2.5
3
3.5
4
WAVE VECTOR (ω_p/c)

Figure 5

V. RESULTS AND DISCUSSION

The room temperature reflectivity of a plane, optically polished sample of InSb ($N = 3.96 \times 10^{17}$) is shown in Fig. 6 for both p and s-polarized light. The angle of incidence is 30°. The data show that the reflectivity is essentially polarization independent. The results differ somewhat from those of McMahon[25] (Fig. 2) taken on the same crystal in that an extra minimum occurs at 183 cm^{-1}. This minimum occurs also (at the same frequency) in another InSb crystal with a concentration of 2.6×10^{17} free carriers per cm^3 but does not appear at all in a sample with a concentration of 1.43×10^{17} free carriers per cm^3. The occurrence of this extra minimum (which is extremely near the TO-mode frequency) is not at all understood. It is possible that the reason this minimum did not show up in one sample is due to a slightly different surface orientation than the (111) orientation specified by the supplier.

Fig. 7 shows the reflectivity of the InSb sample with 3.96×10^{17} donors per cm^3 before and after a 79 line per centimeter grating was cut on the surface. The angle of incidence is 30°. The grating, cut on a spark cutter, has an approximately semicircular profile with diameter 63.5μm separated by a 63.5μm uncut strip as shown in the insert in Fig. 7. The minima for the grating sample, located at 140 and 216 cm^{-1} are in good agreement with the minima predicted if one assumes the spark cutting operation has created a damage layer in which the electron mobility has been greatly reduced (Eqn. 47). This will be discussed in more detail later.

Marschall, Fischer, and Queisser[13] scribed line gratings on optically polished samples of n-type InSb with concentrations ranging from 1 to 7 x 10^{18} electrons per cm^3. The grating spacings (d) varied from 10 to 30 μm. If the incident light is polarized with $\vec{E}$ perpendicular to the grooves, the grating allows the excitation of surface plasmons with wave vectors given by the relation:

$$K = (\omega/c) \sin \theta + 2n\pi/d \tag{48}$$

where θ is the angle of incidence and n is an integer. Their experimental results are shown in Fig. 8. By varying the angle of incidence and the grating spacing, they were able to verify the surface plasmon dispersion relationship (Fig. 4).

Polarization studies were also made on our spark-cut gratings. Fig. 9 shows the reflectivity of a spark-cut grating sample of InSb ($N = 3.96 \times 10^{17}$) with the plane of incidence perpendicular to the grooves at both s and p-polarizations. The angle of incidence was 30°. The first mode (n = 1) for a grating with 5 mil spacing should be (Eqn. 48) at 158 cm^{-1} with successive modes approaching 190 cm^{-1}, the surface plasmon frequency. These modes should show up as reflectivity minima for the p-polarized light but should not be visible for the other polarization. The modes are difficult to observe in Fig. 9.

There are several basic differences between the experiment of

Marschall _et al._ and ours. Their samples were so heavily doped that the plasma frequency was far above the phonon frequencies. Therefore phonon-surface plasmon coupling was not important in their case. Their gratings were finely ruled with a diamond ruling machine thus creating a minimum of surface damage compared to the spark-cut grating surfaces. Because of this absence of a surface damage layer, it is difficult to tell if the high frequency reflection minimum ($\sim 750\ cm^{-1}$ in Fig. 8) occurs at the surface plasmon frequency, which it should by our analysis, or the bulk plasmon frequency since ω_p and ω_{sp} are nearly identical if there is no damage layer (Eqn. 1). Their gratings also did not have the local surface roughness that the spark cutting operation produces which allows the excitation of the large wave vector modes.

An attempt was made to rule a grating using a sharp metal scribe instead of spark cutting in order to extend Marschall's work to samples with lower concentrations where surface plasmon-phonon coupling is important. Fig. 10 shows the reflectivity for both s and p-polarizations of a sample of n-type InSb with 1.43×10^{17} free carriers per cm^3. The grating spacing is 10 mils and the angle of incidence is 30°. The first mode ($n = 1$) using Eqn. 48 should occur at 79 cm^{-1} and the second mode should be at 157 cm^{-1} with successive modes approaching 165 cm^{-1} (ω_{sp}). Because of the low intensity and resulting high noise in the p-polarization data, it is difficult to conclude whether or not surface plasmons have been observed. Our gratings were extremely crude compared to Marschall's gratings which were ruled to 1 per cent accuracy at spacings as small as 10μm. Further work needs to be done with better gratings at these concentrations so that the surface plasmon-phonon-grating interaction can be better understood. Since the minima in Fig. 10 (ω_- and ω_+) are in good agreement with the data of McMahon[25] on the same sample and are not consistent with the surface damage layer theory (Eqn. 47) and spark-cut grating data (Table I), the metal scribe does not produce the thick damage layer that the spark-cutting operation does.

Although we were not successful in studying the second-order grating-surface plasmon interaction in a frequency range where phonon-plasmon coupling is important, we were successful in observing the non-radiative surface modes predicted for a damaged layer-n-type InSb interface (Eq. 47). Returning to Fig. 7, we see that the minima have shifted from 165 and 314 cm^{-1} for the plane sample to 140 and 216 cm^{-1} for the spark-cut samples. The theoretical and experimental values of the minima for the spark cut samples are given in Table I. The theoretical values are from Eqn. 47. The theoretical and experimental values for the plane optically polished samples are also given in Table I. The theoretical values are from Eqn. 5. The results from Table I have also been plotted in Fig. 11. The various crystal parameters necessary to solve Eqn. 5 and Eqn. 47 are given in Table II. The data for the crystal with 2.6×10^{17} free carriers per cm^3 have been interpolated from the other two crystals whose parameters are given by McMahon.[25] The calculated frequencies of the minima for the optically polished samples are those for which $\varepsilon = 0$ (the condition for longitudinal modes), while the experimental frequencies correspond to the reflectivity minima ($\varepsilon = 1$). Hence, the experimentally determined frequencies are not exactly the calculated frequencies. The reflectivities for the spark-cut grating surfaces are essentially independent of both the polarization and the orientation of the plane of incidence with respect to the grating lines (Figs. 9 and 12) which is consistent with the damage layer-InSb interface model discussed in Chapter IV.

Eqn. 14, the relationship between ω_{sp} and ω_p, was derived assuming an infinitely thick dielectric external to the sample. This approxmiation is probably valid for thicknesses greater than a wavelength (~ .01cm) but, as the thickness decreases, ε will approach one and ω_{sp} will approach ω_p. This suggests that as the thickness of the damage layer is decreased, the reflectivity of the surface plasmon-phonon system (Fig. 7) should approach the reflectivity of the coupled, bulk plasmon-longitudinal optical phonon system. The spark-cut grating surfaces were etched to study this dependence of the reflectivity on the thickness of the surface damage layer. The echant used was composed of equal parts of CP-4, acetic acid, and water. Fig. 13 shows the reflectivity after successive etches. The results are in agreement with the above analysis. After about .01 cm of material had been etched away, the reflectivity returned to that of the the polished samples although there was very little change in the depth of the grating lines.

TABLE I

REFLECTIVITY MINIMA FOR BOTH PLANE AND GRATING SAMPLES OF InSb

(±5 wave numbers)

Concentration ($10^{17}/cm^3$)		ω_- (cm^{-1})		ω_+ (cm^{-1})	
		Exp.	Theo.	Exp.	Theo.
1.43	Plane	162	142	237	216
	Grating	125	105	215	207
2.60	Plane	160	170	264	244
	Grating	130	137	212	214
3.96	Plane	165	180	314	284
	Grating	140	159	216	227

TABLE II

VARIOUS CRYSTAL PARAMETERS OF THE InSb SAMPLES STUDIED

CONCENTRATION ($10^{17}/cm^3$)	TO-FREQUENCY (cm^{-1})	EFFECTIVE MASS RATIO	ELECTRON DAMPING (cm^{-1})	PHONON DAMPING (cm^{-1})
1.43	181.5	.03	9.8	3.8
2.60	181.5	.03	13.0	4.0
3.96	181.5	.031	16.2	4.2

FIGURE 6

REFLECTANCE VERSUS WAVE NUMBER OF A POLISHED CRYSTAL OF InSb ($N=3.96 \times 10^{17}$) FOR BOTH S AND P-POLARIZATIONS. The solid line is for the s-polarized light while the dotted line is for the p-polarization. The angle of incidence is 30°.

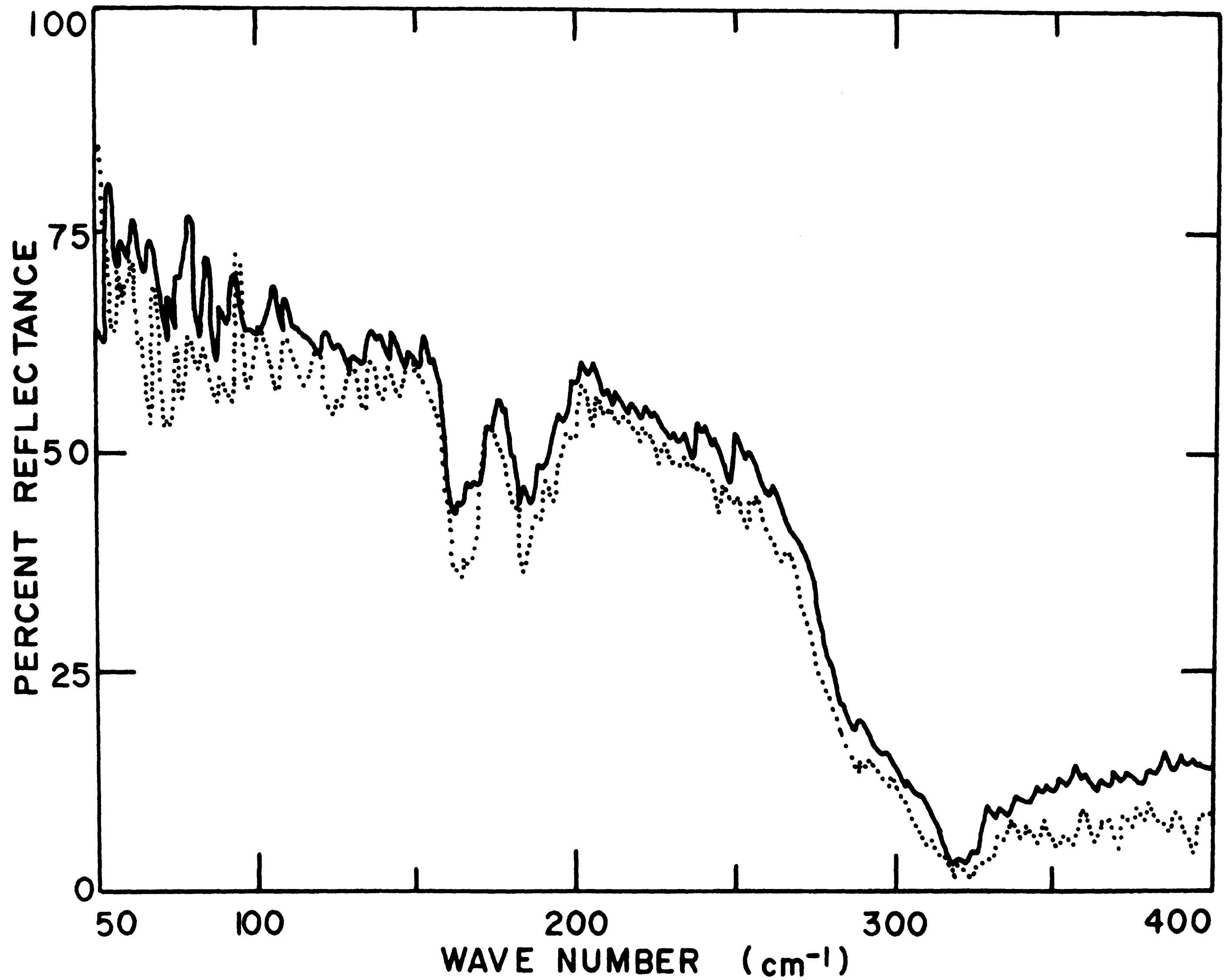
100
75
50
25
0
PERCENT REFLECTANCE
50
100
200
300
400
WAVE NUMBER (cm^{-1})

Figure 6

FIGURE 7

REFLECTANCE VERSUS WAVE NUMBER FOR A POLISHED CRYSTAL OF InSb ($N=3.96\times10^{17}$) BEFORE AND AFTER A GRATING WAS SPARK CUT ON THE SURFACE. The solid line is for the polished surface while the dotted line is for the spark-cut surface. The angle of incidence is 30°. The grating spacing is 127 μm. The insert shows the approximate grating profile.

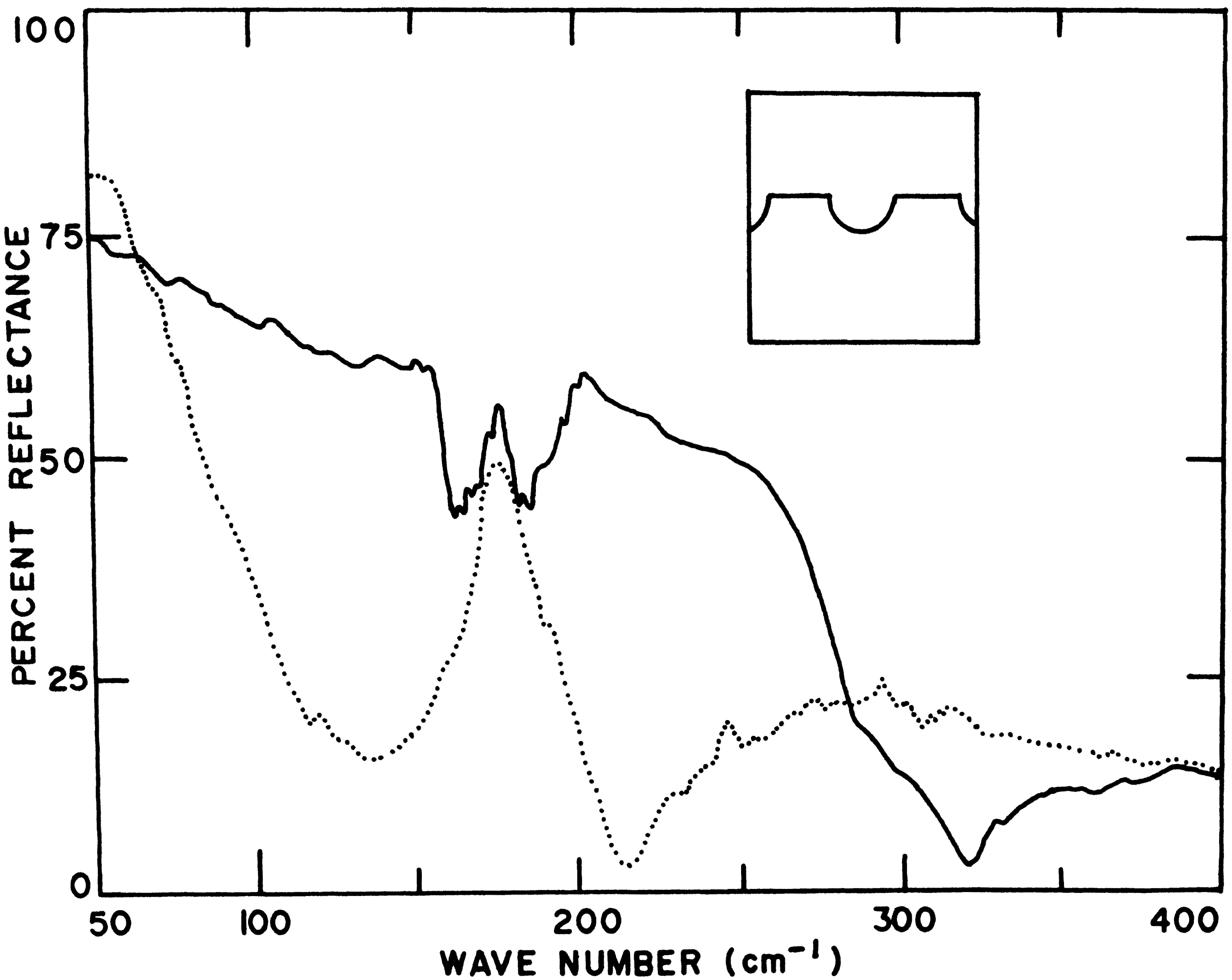
100
75
50
25
0
PERCENT REFLECTANCE
50
100
200
300
400
WAVE NUMBER (cm^{-1})

Figure 7

FIGURE 8

REFLECTANCE VERSUS WAVE NUMBER OF A POLISHED CRYSTAL OF InSb ($N=7x10^{18}$) WITH A GRATING INSCRIBED ON THE SURFACE. The figure is from Marschall, Fischer and Quiesser.[13] The grating spacing is 30μm. The angle of incidence is 0°. The arrows show the first, second and third-order (Eqn. 48) surface plasmon frequencies. The dashed line is the reflectivity before the grating was inscribed on the surface.

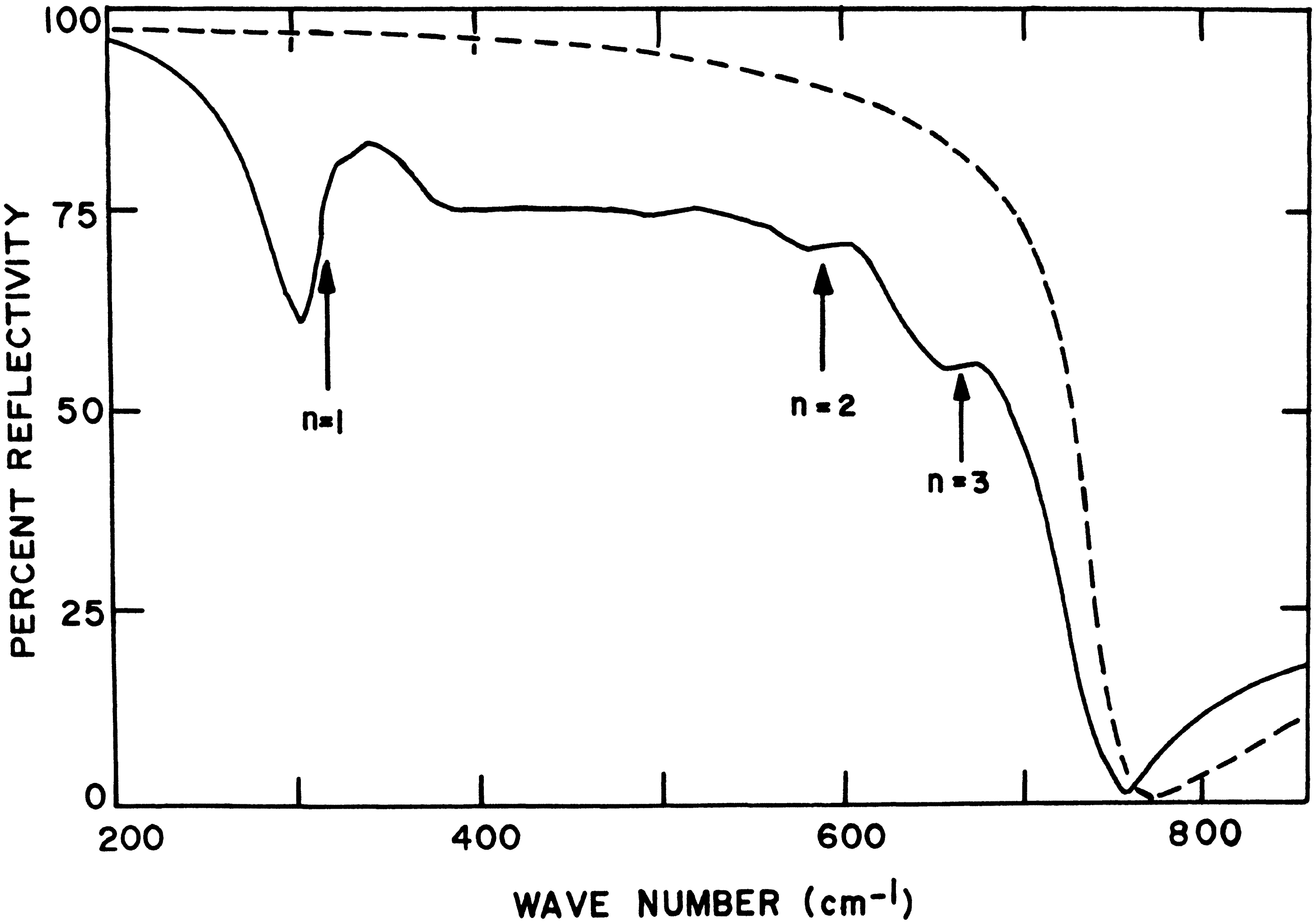
100
75
50
25
0
PERCENT REFLECTIVITY
n=1
n=2
n=3
200
400
600
800
WAVE NUMBER (cm⁻¹)

Figure 8

FIGURE 9

REFLECTANCE VERSUS WAVE NUMBER OF A SPARK-CUT GRATING SAMPLE OF InSb ($N=3.96 \times 10^{17}$) AT BOTH S AND P-POLARIZATIONS. The solid line is for the s-polarization and the dashed line is for the p-polarization. The angle of incidence is 30°. The grating spacing is 127 μm. The plane of incidence is perpendicular to the grating lines.

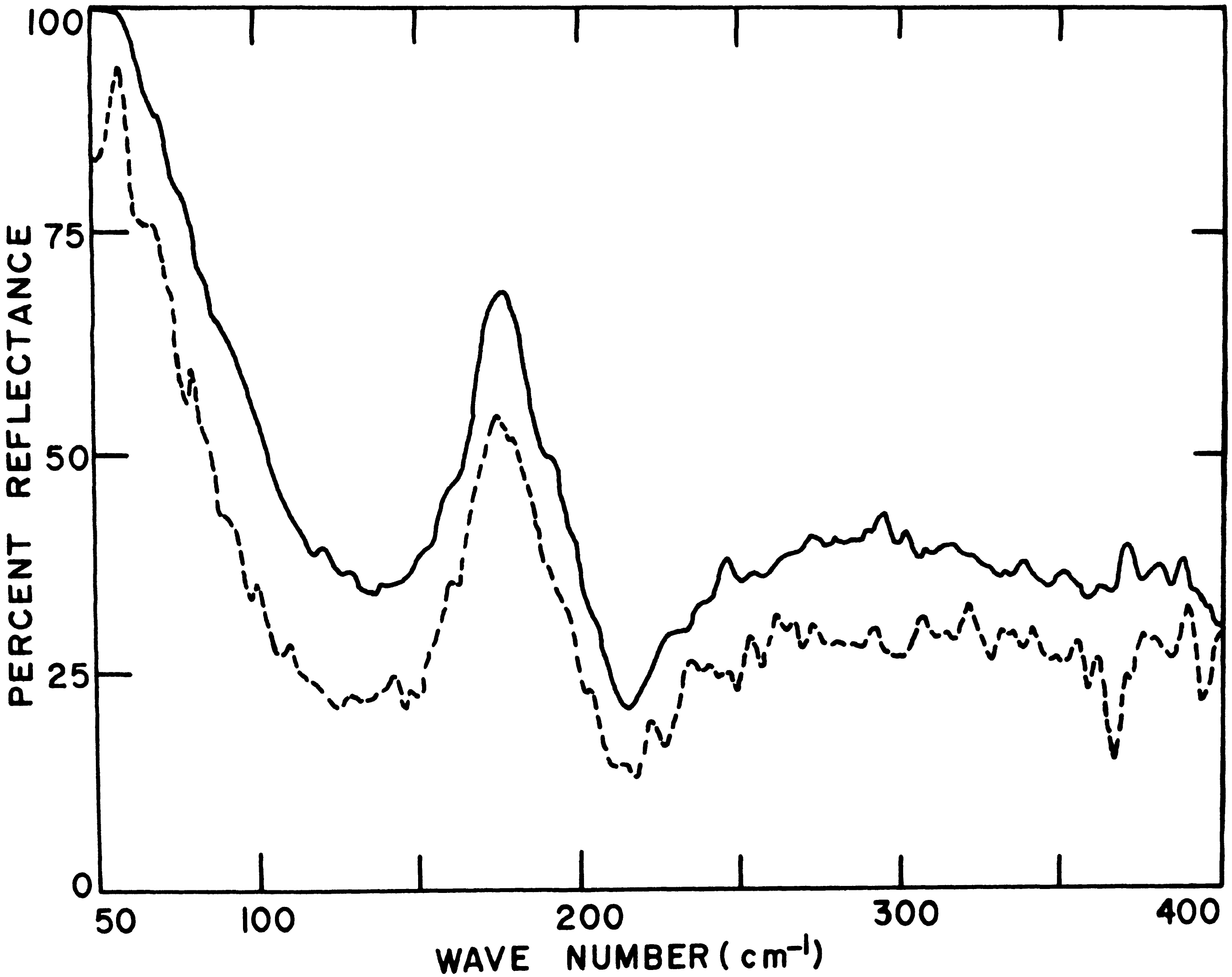

PERCENT REFLECTANCE
100
75
50
25
0
50
100
200
300
400
WAVE NUMBER (cm⁻¹)

Figure 9

FIGURE 10

REFLECTANCE VERSUS WAVE NUMBER OF A POLISHED CRYSTAL OF InSb ($N=1.43\times10^{17}$) WITH A GRATING INSCRIBED ON THE SURFACE AT BOTH S AND P-POLARIZATIONS. The grating spacing is 254 μm. The angle of incidence is 30°. The solid line is for the s-polarization while the dashed line is for the p-polarization. The plane of incidence is perpendicular to the grating lines.

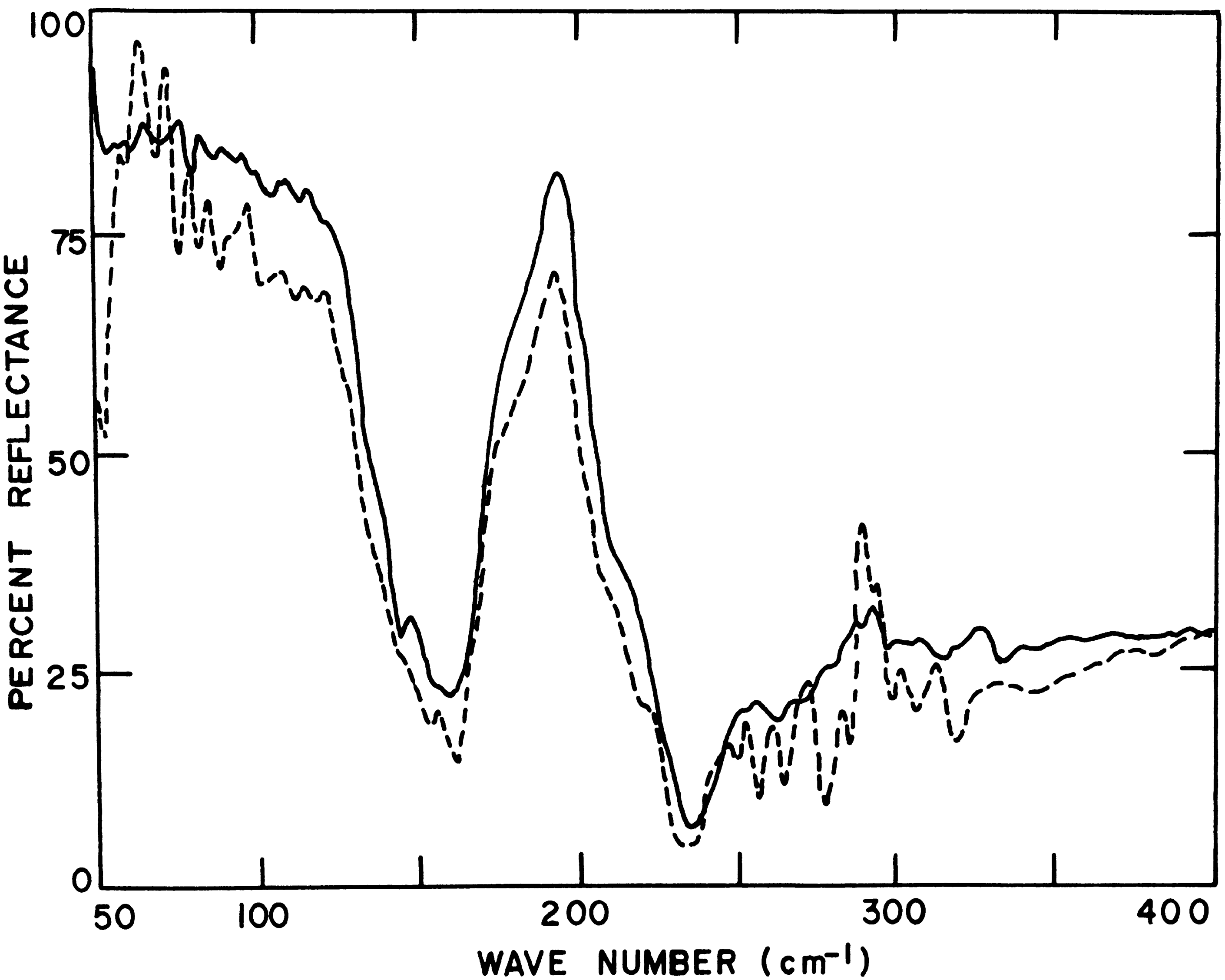
100
75
50
25
0
PERCENT REFLECTANCE
50
100
200
300
400
WAVE NUMBER (cm⁻¹)

Figure 10

FIGURE 11

FREQUENCY OF NORMAL MODES VERSUS CONCENTRATION FOR BOTH POLISHED AND SPARK-CUT GRATING SURFACES OF InSb. The x's and solid curves are the experimental and calculated normal modes for the polished samples while the dots and dashed curves are for the spark-cut grating samples. The frequency is labeled in units of ω_L (the longitudinal optical phonon frequency) while the concentration is labeled in units of ω_P^2/ω_L^2.

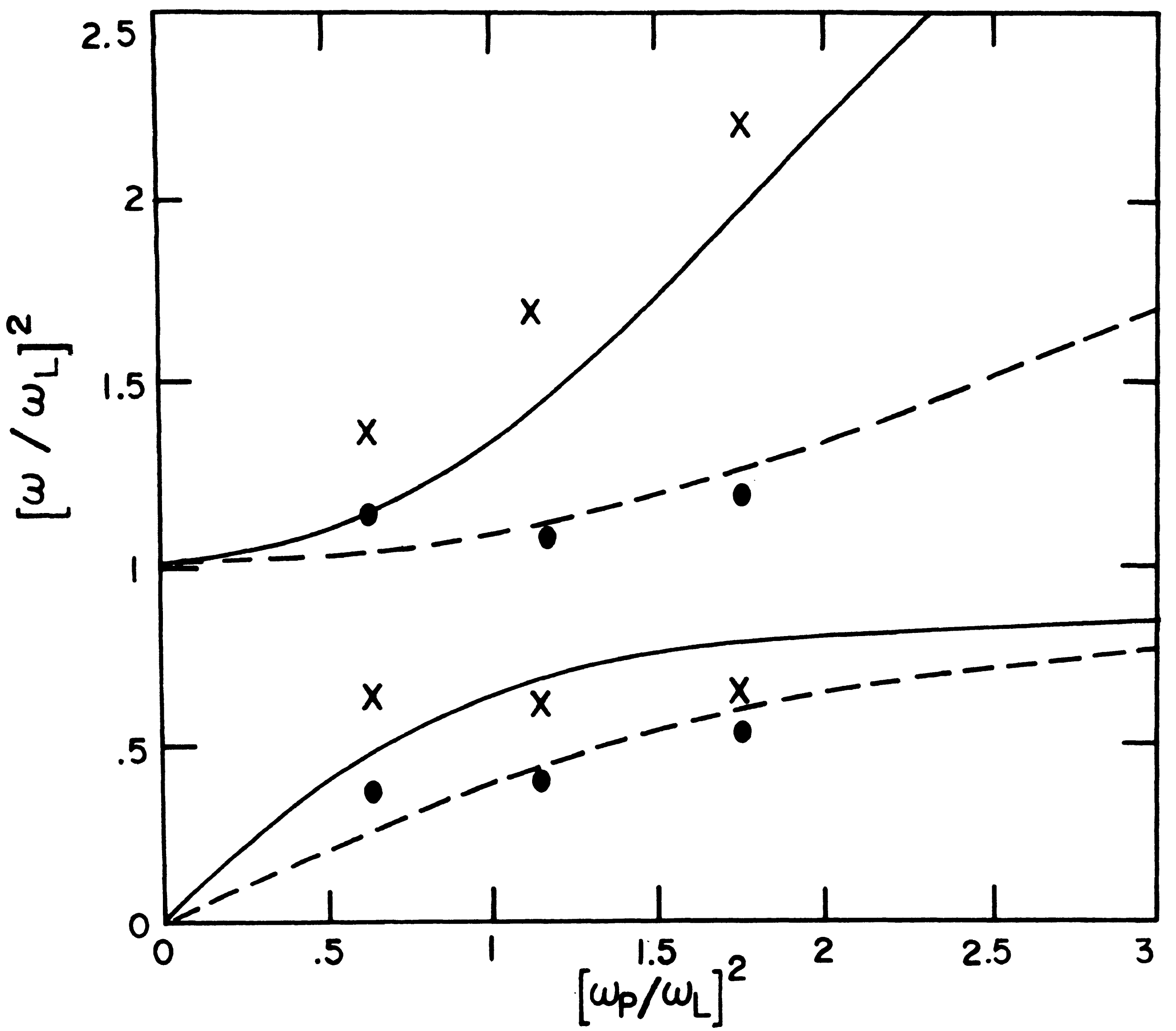

Figure 11

FIGURE 12

REFLECTANCE VERSUS WAVE NUMBER OF A SPARK-CUT GRATING SURFACE OF InSb ($N=3.96 \times 10^{17}$) WITH THE PLANE OF INCIDENCE BOTH PARALLEL AND PERPENDICULAR TO THE GRATING LINES. The solid line is for the plane of incidence perpendicular to the grating lines while the dashed line is for the plane of incidence parallel to the grating lines. The angle of incidence is 30°. The light is polarized with $\vec{E}$ perpendicular to the plane of incidence.

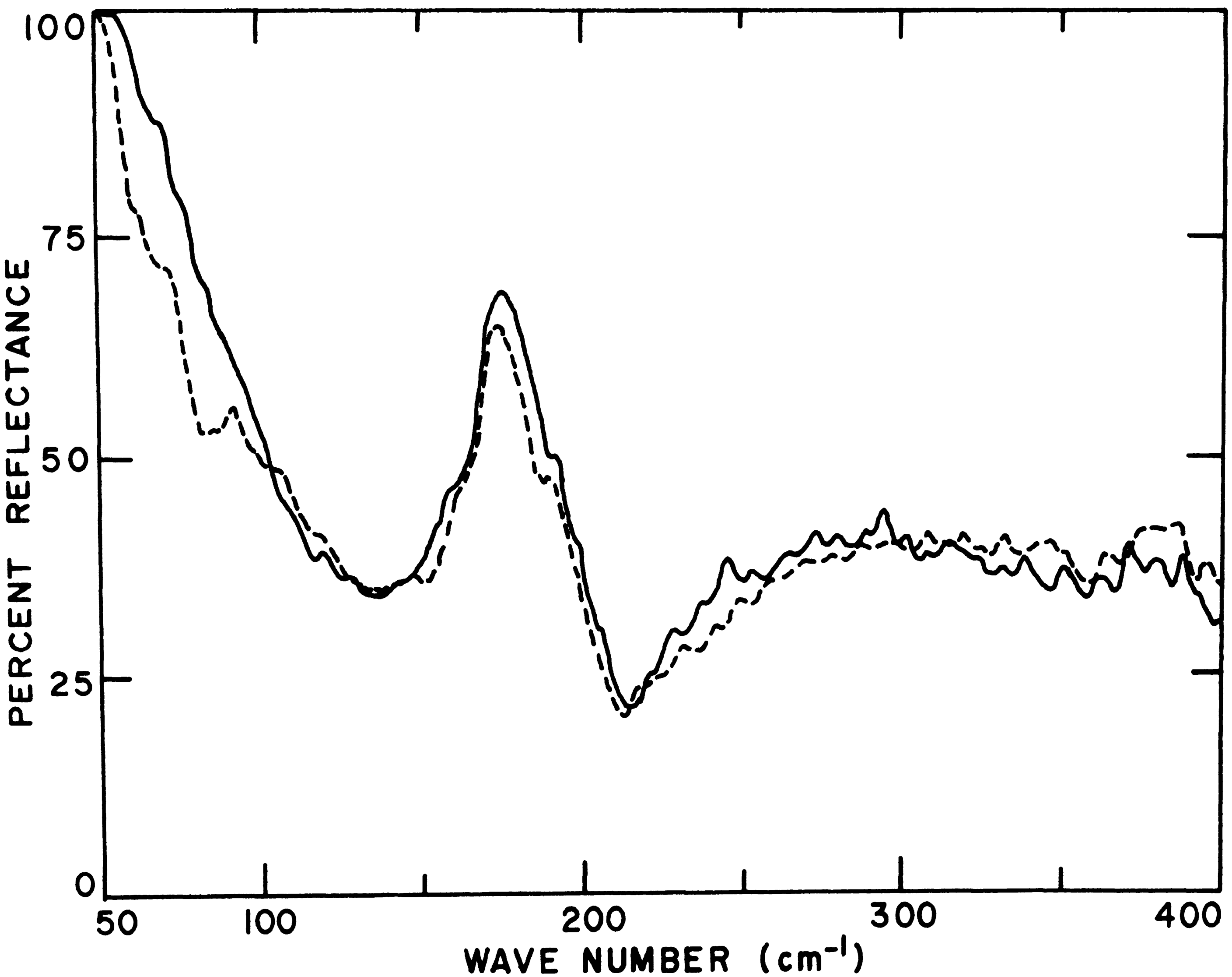

PERCENT REFLECTANCE
100
75
50
25
0
50
100
200
300
400
WAVE NUMBER (cm^{-1})

Figure 12

FIGURE 13

REFLECTANCE VERSUS WAVE NUMBER OF A SPARK-CUT GRATING SURFACE ($N=3.96\times10^{17}$) AFTER VARIOUS ETCH TIMES. The dash-dotted line, 57 sec etch time; dotted line, 12 sec etch time; dashed line, 6 sec etch time; solid line, no etching. The angle of incidence is 30°. The plane of incidence is perpendicular to the grating lines.

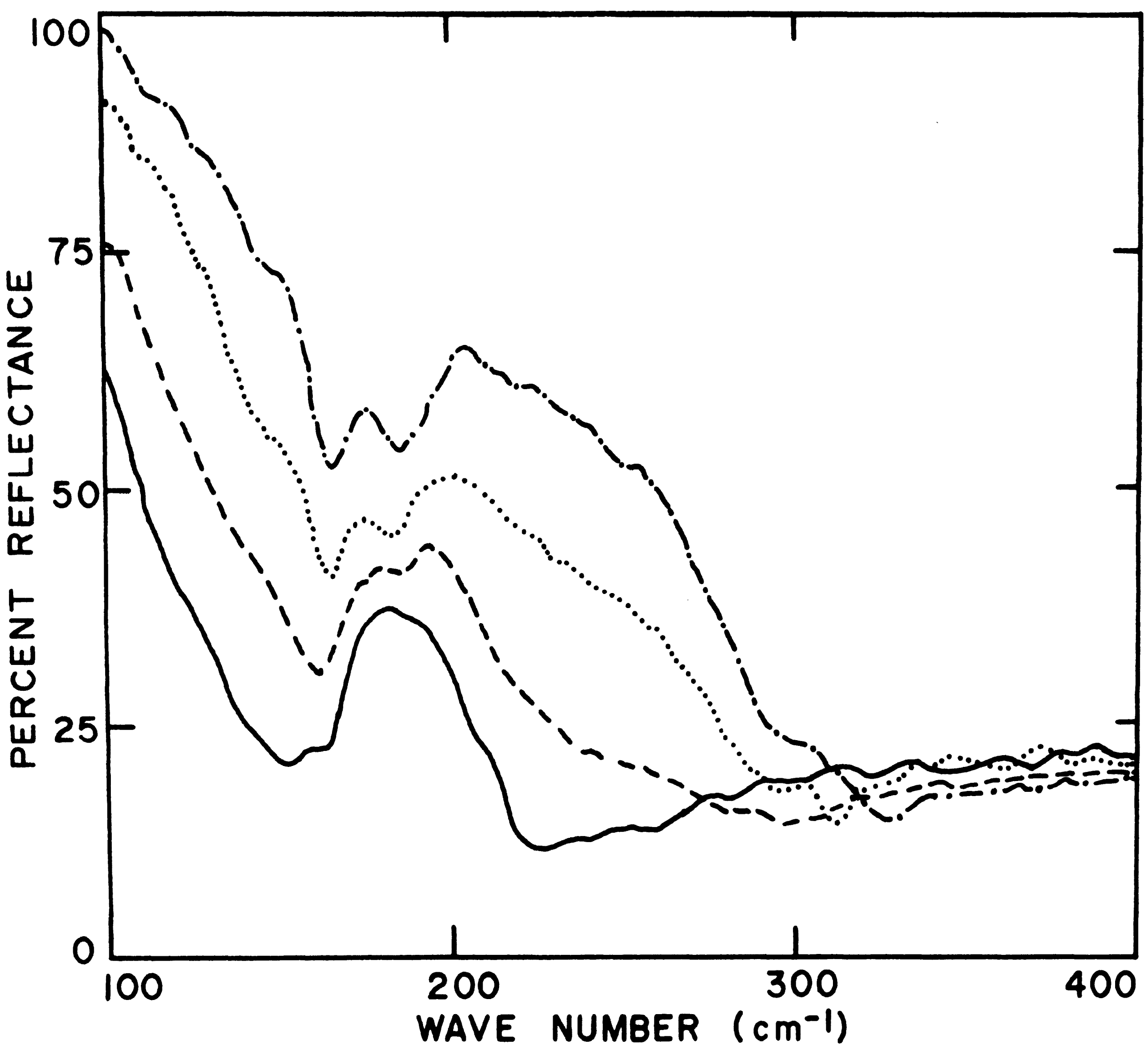

100
75
50
25
0
PERCENT REFLECTANCE
100
200
300
400
WAVE NUMBER (cm⁻¹)

Figure 13

VI. CONCLUSION

The far infrared reflectivity of n-type InSb has been studied. Results suggest that samples with a sufficiently thick depletion layer (or damage layer) show effects due to surface plasmons. If the surface plasmon frequency is near the phonon frequencies, coupling between these two independent elementary excitations becomes important. The results agree qualitatively with a proposed model for the coupling.

Future work might include a study of the angular distribution of the radiation scattered by the surface plasmon-phonon system. The use of a prism to excite surface plasmons in polished samples by frustrated total reflection has been proposed by Otto.[30] This would allow a study of the coupling of the surface plasmons to the surface optical phonons.

BIBLIOGRAPHY

1. R. H. Ritchie, Phys. Rev. 106, 874 (1957).

2. C. J. Powell and J. B. Swan, Phys. Rev. 115, 869(1959).

3. H. Boersch, P. Dobberstein, D. Fritzsche, and G. Sauerbrey, Z. Phys. 187, 97 (1965).

4. G. E. Jones, L. S. Cram, and E. T. Arakawa, Phys. Rev. 147, 515 (1966).

5. S. N. Jasperson and S. E. Schnatterly, Phys. Rev. 188, 759 (1969).

6. J. L. Stanford, J. Opt. Soc. Am. 60, 49 (1970).

7. O. Hunderi and D. Beaglehole, Bull. Am. Phys. Soc. 14, 26 (1969).

8. R. W. Wood, Phil. Mag. 4, 396 (1902).

9. R. H. Ritchie, E. T. Arakawa, J. J. Cowan, and R. N. Hamm, Phys. Rev. Lett. 21, 1530 (1968).

10. D. C. Tsui, Phys. Rev. Lett. 22, 293 (1969).

11. K. L. Ngai, E. N. Economou, and M. H. Cohen, Phys. Rev. Lett. 22, 1375 (1969).

12. K. L. Ngai and E. N. Economou, Phys. Rev. B4, 2132 (1971).

13. N. Marschall, B. Fischer, and H. J. Queisser, Phys. Rev. Lett. 27, 95 (1971).

14. A. Mooradian and G. B. Wright, Phys. Rev. Lett. 16, 999 (1966).

15. B. Tell and R. J. Martin, Phys. Rev. 167, 381 (1968).

16. C. G. Olson and D. W. Lynch, Phys. Rev. 177, 1231 (1969).

17. T. J. McMahon and R. J. Bell, Phys. Rev. 182, 526 (1969).

18. B. B. Varga, Phys. Rev. 137, A1896 (1965).

19. K. S. Singwi and M. P. Tosi, Phys. Rev. 147, 658 (1966).

20. W. E. Anderson, R. W. Alexander, and R. J. Bell, Phys. Rev. Lett. 27, 1057 (1971).

21. W. F. Parks. Private Communication. June, 1971.

22. K. W. Chiu and J. J. Quinn, Phys. Lett. 35A, 469 (1971).

23. R. F. Wallis and J. J. Brion, Solid State Communications (To Be Published).

24. D. Pines, Elementary Excitations in Solids, W. A. Benjamin, New York (1964).

25. T. J. McMahon, Thesis (University of Missouri-Rolla, 1969) Unpublished.

26. R. A. Ferrell, Phys. Rev. 111, 1214 (1958).

27. K. R. Symon, Mechanics, Addison-Wesley, Reading, Mass. p.190 (1964).

28. E. A. Stern and R. A. Ferrell, Phys. Rev. 120, 130 (1960).

29. R. Fuchs and K. L. Kliewer, Phys. Rev. B3, 2270 (1971).

30. A. Otto, Z. Phys. 216, 398 (1968).

VITA

The author, William Eugene Anderson, was born on August 28, 1946, in Minneapolis, Minnesota. He received his primary and secondary education in Richfield, Minnesota. He received a Bachelor of Physics Degree from the University of Minnesota in June 1968. He received a Master of Science Degree in Physics from the University of Missouri-Rolla in Rolla, Missouri in June 1970.

He has been enrolled in the Graduate School of the University of Missouri-Rolla since September 1968. He was a teaching assistant from September 1968 to June 1969 and since September 1969 he was a research assistant supported by the Air Force Office of Scientific Research.